The Role of Northern Lakes in a Regional Energy Balance

WAYNE R. ROUSE,* CLAIRE J. OSWALD,* JACQUELINE BINYAMIN,* CHRISTOPHER SPENCE,+
WILLIAM M. SCHERTZER,# PETER D. BLANKEN,@ NORMAND BUSSIÈRES,& AND CLAUDE R. DUGUAY**

*School of Geography and Geology, McMaster University, Hamilton, Ontario, Canada
+Environment Canada, Yellowknife, Northwest Territories, Canada
#National Water Research Institute, Burlington, Ontario, Canada
@Department of Geography, University of Colorado, Boulder, Colorado,
&Meteorological Service of Canada, Toronto, Ontario, Canada
**Geophysical Institute, University of Alaska Fairbanks, Fairbanks, Alaska

(Manuscript received 6 May 2004, in final form 2 December 2004)

ABSTRACT

There are many lakes of widely varying morphometry in northern latitudes. For this study region, in the central Mackenzie River valley of western Canada, lakes make up 37% of the landscape. The nonlake components of the landscape are divided into uplands (55%) and wetlands (8%). With such abundance, lakes are important features that can influence the regional climate. This paper examines the role of lakes in the regional surface energy and water balance and evaluates the links to the frequency–size distribution of lakes. The primary purpose is to examine how the surface energy balance may influence regional climate and weather. Lakes are characterized by both the magnitude and temporal behavior of their surface energy balances during the ice-free period. The impacts of combinations of various-size lakes and land–lake distributions on regional energy balances and evaporation cycles are presented. Net radiation is substantially greater over all water-dominated surfaces compared with uplands. The seasonal heat storage increases with lake size. Medium and large lakes are slow to warm in summer. Their large cumulative heat storage, near summer's end, fuels large convective heat fluxes in fall and early winter. The evaporation season for upland, wetland, and small, medium, and large lakes lasts for 19, 21, 22, 24, and 30 weeks, respectively. The regional effects of combinations of surface types are derived. The region is initially treated as comprising uplands only. The influences of wetland, small, medium, and large lakes are added sequentially, to build up to the energy budget of the actual landscape. The addition of lakes increases the regional net radiation, the maximum regional subsurface heat storage, and evaporation substantially. Evaporation decreases slightly in the first half of the season but experiences a large enhancement in the second half. The sensible heat flux is reduced substantially in the first half of the season, but changes little in the second half. For energy budget modeling the representation of lake size is important. Net radiation is fairly independent of size. An equal area of medium and large lakes, compared with small lakes, yields substantially larger latent heat fluxes and lesser sensible heat fluxes. Lake size also creates large differences in regional flux magnitudes, especially in the spring and fall periods.

1. Introduction

Lakes of various sizes are ubiquitous in high-latitude subarctic and tundra regions. In the central Mackenzie River valley of western Canada, from which most of the data used in this study are derived (Fig. 1), there are about 32 370 lakes. For the whole Mackenzie River basin, a surface area for lakes of 144 000 km^2 has been determined from the Canada Center for Remote Sensing (CCRS-2) land cover classification (Bussières 2002). This represents about 8% of the basin. However, if more recently available CCRS water fraction data are used, the estimated lake coverage approaches 11%. In the northern Hudson Bay Lowland, Bello and Smith (1990) estimate the coverage of lakes at 41% of the landscape. In flat wetland terrain it is often difficult to distinguish between wetlands and lakes, because there are no precise boundaries to the lakes (Rouse et al. 1997). Other circumpolar high-latitude regions such as Alaska, northern Scandinavia, and northern Russia exhibit this substantial areal coverage by lakes.

The study area extends from mid–Great Slave Lake northward, and incorporates a 50 000-km^2 area (Fig. 1; Table 1). It was chosen for a number of reasons. It is positioned centrally within the Mackenzie River basin. The terrain is typical of the Canadian Shield, with uplands of exposed bedrock and dry land vegetation, wetlands, many lakes, and a large variety in lake sizes. An

Corresponding author address: Dr. Wayne Rouse, School of Geography and Geology, McMaster University, Hamilton, ON L8S 4K1, Canada.
E-mail: rouse@mcmaster.ca

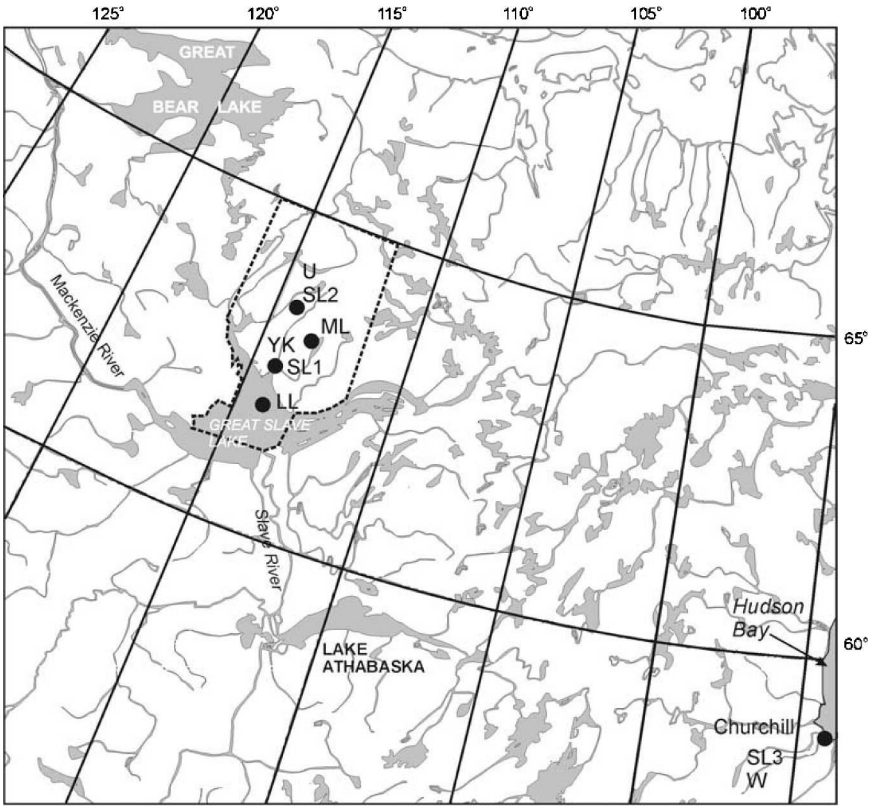

FIG. 1. The location of the research area and measurement sites. YK is city of Yellowknife; U is upland; W is wetland; SL1, SL2, and SL3 are small lakes; ML is the medium lake; and LL is the large lake. The dashed line denotes the region of this study.

in-depth analysis of lake sizes and frequencies for the region has been completed. Four lakes that have been studied intensively over the past decade are placed centrally within this study region. The region includes the main basin of Great Slave Lake. This is important since large lakes are an important regional component of the Mackenzie River basin. Other notably large lakes in the basin are Great Bear Lake to the north and Lake Athabaska to the south. Only the main basin of Great Slave Lake is chosen since the inclusion of the East Arm would bias the regional representation of large lake area to the high side.

Because of their abundance, lakes are important features in the regional climate. This paper examines the regional role of lakes in the surface energy balance. It links this to the frequency–size distribution of lakes. Our study examines how lakes of different sizes influence the seasonality in the surface energy balance. It also considers how this may influence the regional climate.

TABLE 1. The area and percent cover of the surface types in the study region bounded by 62°–65°N and 112°–116°W (Fig. 1).

Surface type	Symbol	Area (km^2)	% Landscape
Uplands	U	27 269	55
Wetlands	W	4067	8
Small lakes (<1 km^2)	SL	3706	7
Medium lakes (1–100 km^2)	ML	5632	11
Large lakes (>100 km^2)	LL	9326	19
Total		50 000	100

We employ recently gathered data from northern lakes of various sizes. The role of different-size lakes in the regional radiation balance and heat and water vapor exchanges with the atmosphere is characterized and quantified. The regional energy balance is initially calculated for an upland-only scenario. The influence of wetlands and different-size lakes is then added sequentially, building up to the known regional landscape. The analysis focuses on the combined thaw season of terrestrial surfaces and open-water period of lakes.

The lakes employed in this study range from less than a meter in depth to Great Slave Lake, which is one of the largest and deepest freshwater lakes in the world. The smaller, shallower lakes have an energy cycle as follows: In late winter, thaw of the ice and its snow cover is not significant until air temperatures exceed freezing. The onset of thaw normally coincides with long daylight periods in spring. The albedo is dramati-

cally reduced because of the melting of the overlying snow cover and ponding of water on the frozen lake surfaces. Melting can proceed rapidly with a combination of above-freezing temperatures and strong absorption of solar radiation. As snow disappears and the ice cover thins, solar radiation penetrates the water beneath. Upon final thaw, solar heating of the shallow lakes raises their temperatures rapidly. This allows vigorous evaporation to proceed early in the thaw season. The heating and cooling of shallow lakes is subsequently governed by the temperature of the overlying air masses. With cold overlying air, the latent and sensible heat fluxes are large and shallow lakes cool rapidly (Petrone and Rouse 2000). With warm overlying air, vertical temperature and humidity gradients are suppressed, sensible and latent heat fluxes are dampened, and lakes warm. Subfreezing temperatures in early winter coincide with short daylight periods. Freeze-up can occur quickly. The initial formation of ice puts an effective lid on outgoing turbulent heat fluxes, and the shallow lake evaporation cycle ends. In subarctic latitudes, the period of substantive evaporative and sensible heat loss from shallow lakes is on the order of 4 months (Rouse et al. 2002). This becomes less in more northerly regions.

Large, deep, high-latitude lakes, such as Great Slave Lake, Great Bear Lake, and Lake Athabaska, have a thermal and energy cycle that can be represented by Great Slave Lake (Rouse et al. 2003; Schertzer et al. 2003). The thermal cycle shows a winter minimum in temperature and heat storage, a spring heating period, a summer period of maximum heat storage, and a fall–winter cooling phase. Annual heat content is comparable to the lower Laurentian Great Lakes such as Lakes Ontario, Huron, and Michigan (Schertzer 1997). The time of ice breakup in Great Slave Lake ranges from late May to late June. Freeze-back occurs from late November to the end of December. This gives an average ice-free period of 170 days (Walker et al. 2000).

During thaw, and especially during freeze-back, open areas of large lakes exchange heat through evaporation and sensible heat loss. Great Slave Lake becomes isothermal in early October at approximately 8°–9°C. Its surface layers cool to the 4°C temperature of maximum density in mid- to late October. At this time it undergoes thermally induced vertical overturning. It then experiences a 4-month period of near-freezing beneath-ice temperatures (Schertzer et al. 2000). During spring, the total heat flux is dominated by high net radiation that contributes primarily to lake heating (Schertzer et al. 2000). Heating proceeds slowly because of the large vertical mass and deep thermal mixing, particularly during storms. After the exchange of surface and deep waters at 4°C the development of thermal stratification proceeds. During this heating phase the turbulent heat fluxes are often negative, responding to thermal inversions (Blanken et al. 2000). Positive fluxes usually do not commence until mid-July.

The maximum surface temperature of Great Slave Lake varies from 17° to 25°C (Bussières 2002). At these temperatures the entire lake is freely evaporating to the overlying atmosphere. There is a strong asymmetry between heating and cooling rates. Heat storage is large in spring and summer. During fall and early winter there is increased evaporation and sensible heat flux with the warm surface waters exchanging both heat and mass with the cold overlying air (Rouse et al. 2003). This large heat exchange continues as long as there is open water. A complete winter ice and snow cover effectively restricts heat and mass exchanges. Evaporation from Great Slave Lake operates over a period ranging from 5 to 6 months.

Because they strongly absorb solar radiation and provide a continuously wet surface, lakes of all sizes have large seasonal evaporation amounts (Eaton et al. 2001; Rouse et al. 2002). Weather conditions that result in high temperature and large solar radiation can increase annual evaporation from a shallow lake by more than 50% and from Great Slave Lake by more than 30%. Shallow lakes warm quickly in spring and maintain high evaporation rates until they freeze in fall. Larger and deeper lakes take substantial periods to thaw and warm. However, they stay thawed into late fall or early winter. Their total evaporation amounts are significantly greater than for other high-latitude surfaces studied (Rouse et al. 2002).

The frequency and size of lakes substantially influence the magnitude and timing of regional evaporative and sensible heat inputs to the atmosphere. This makes them important to regional climatic and meteorological processes.

2. Methods

a. Surface energy balance

The one-dimensional surface energy balance for land is given by

$$Q^* = Q_E + Q_H + Q_G, \tag{1}$$

where Q^* is net radiation, Q_E is the latent heat flux (evaporative heat flux), Q_H is the sensible heat flux, and Q_G is the heat exchange with the substrate.

Net radiation is fundamental to evaluating surface differences in the energy balance of different surface types and is examined in terms of its component fluxes

$$Q^* = K\downarrow - K\uparrow + L\downarrow - L\uparrow = K\downarrow(1 - \alpha) + L\downarrow - L\uparrow. \tag{2}$$

Here $K\downarrow$ and $K\uparrow$ are incoming and reflected solar radiation, $L\downarrow$ and $L\uparrow$ are incoming and outgoing longwave radiation, and α is surface albedo. Net solar radiation $K^* = K\downarrow - K\uparrow$ and net longwave radiation $L^* = L\downarrow - L\uparrow$.

TABLE 2. The average size of lakes shown in Fig. 2 is indicated. Small, medium, and large lakes used in this study are designated SL, ML, and LL, respectively. The lake size categories are SL (0–1 km^2), ML (1–100 km^2), and LL (>100 km^2). Data for other medium lakes in the region (M1 . . . M4) are adapted from Bussières and Schertzer (2003), and these are averaged to give M (Ave). ND signifies that the lake depths are unknown.

Lakes	Latitude (°N)	Area (km^2)	Average depth (m)	Years of data
SL	61.6	0.10	1.6	7
ML	62.9	5.5	12.1	3
M1 Gordon	63.1	154	ND	1
M2 Duncan	62.9	16	ND	1
M3 Prelude	62.6	18	ND	1
M4 Francois	62.4	13	ND	1
M (Ave)	62.5	50	ND	1
LL	61.9	18 500	32.2	5

For a lake during the thaw season, the one-dimensional energy balance is given by

$$Q^* = Q_E + Q_H + Q_S + Q_{GL}. \quad (3)$$

Heat storage in lakes, Q_S, is normally an order of magnitude larger than Q_{GL}, the heat conduction across the lake bottom. Most of the heat entering a lake is through the absorption of solar radiation. Its magnitude is large because surface albedo is small. Solar radiation can penetrate deeply. As a result, clear-water lakes can warm deeply. This deep warming is augmented by wind-driven convective mixing and free convective mixing. The combination of depth of penetration of solar radiation and deep mixing determines the depth of the mixing layer. The surface convective heat exchanges with the atmosphere, Q_E and Q_H, are driven primarily by the vertical temperature and vapor-pressure gradients, dT/dz and de/dz, in which T is temperature, e is vapor pressure, and z is height above the surface.

Large lakes differ from land surfaces because, on a daily and even weekly basis, the surface fluxes often do not correspond in magnitude to the solar or net radiation regimes. Because of their large heat storage capacity, large lakes can lose heat and water vapor almost as readily at night as during the day, and more readily in late summer and fall than in spring and early summer (Rouse et al. 2003). They are very responsive to the characteristics of the overlying air. If a warm, relatively calm, and sunny period is followed by a cold, dry air mass and cloudy, windy conditions, the convective and latent heat fluxes can increase dramatically, even if there is no direct solar input. This arises because dT/dz and de/dz grow large, and both buoyant and mechanical convection are large (Blanken et al. 2003).

Lake sizes are defined in Table 2. Small lakes (0–1 km^2) are shallow (average depths <5 m in depth). Medium (1–100 km^2) and large (>100 km^2) lakes have average depths ranging from >5 to 70+ m. The heat storage in lakes, Q_S, has been determined using calorimetric techniques

$$Q_S = C_W \Delta T_W/\Delta t, \quad (4)$$

where C_W is the heat capacity of water. The temperature change with time, $\Delta T_W/\Delta t$, is integrated over the total depth of the lake. For shallow lakes, the heat flux across the lake bottom is determined as

$$Q_{GL} = K_W \Delta T_B/\Delta z, \quad (5)$$

where K_W is the thermal conductivity of the bottom sediments and $\Delta T_B/\Delta z$ is the average vertical temperature gradient measured across those sediments. For deep lakes Q_{GL} is ignored since the sun cannot penetrate to the lake bottom (Worth 2002) and the bottom water temperature undergoes almost no seasonal change (Schertzer et al. 2000).

In this study, the energy balances have been determined using the Bowen ratio energy balance (BREB) approach (Eaton et al. 2001; Oswald and Rouse 2004) and eddy covariance (Blanken et al. 2000; Spence and Rouse 2002) methods.

The BREB approach derives from the surface energy balance and flux-gradient relationships for latent and sensible heat giving,

$$Q_E = \frac{Q^* - \Delta Q_S}{\beta + 1} \quad (6)$$

$$Q_H = \beta Q_E. \quad (7)$$

Here ΔQ_S is the net storage of heat in the substrate. The Bowen ratio, β, is the ratio of the sensible heat flux to the latent heat flux and can be expressed in terms of the gradients of air temperature and vapor pressure as

$$\beta = \gamma \frac{\partial T}{\partial e}, \quad (8)$$

where γ is the psychrometer constant.

Eddy covariance is a direct measurement of the latent and sensible heat fluxes:

$$Q_E = L_v w' \rho v', \quad (9)$$

$$Q_H = C_a w' T', \quad (10)$$

where L_v and C_a are the latent heat for vaporization of water and heat capacity of air, respectively, and $w'\rho v'$ and $w'T'$ are the eddy covariances of vertical wind and water vapor concentration and vertical wind and air temperature, respectively.

b. Land and lake data used in this study

This study concentrates on a 50 000-km^2 sector of Canadian Shield that includes the northern half of the main basin of Great Slave Lake and extends northward to near the southern shore of Great Bear Lake (Fig. 1). It is bounded in the east–west direction by longitudes 112° and 116°W. Within this sector, upland terrain and Great Slave Lake compose the largest surface areas, with the remainder fairly equally divided between wetlands, small, and medium lakes (Table 1).

TABLE 3. A description of the sources of data that have been used in this study. Symbols denote the following: U—upland Canadian Shield terrain; W—wetland; SL1—small lake 1; SL2—small lake 2; SL3—small lake 3; M—medium lake; LL—large lake; EC—eddy covariance; BREB—Bowen ratio energy budget; Ref—reference sources for studies: 1) Spence and Rouse (2002); 2) Eaton et al. (2001); 3) Rouse et al. (2002); 4) Boudreau and Rouse (1995); 5) Spence et al. (2003); 6) Blanken et al. (2000); 7) Rouse et al. (2003); 8) Schertzer (2000).

Site	Lat	Lon	EB methods	Lake area (km^2)	Avg lake depth (m)	Data years	Ref
U	63°35′N	113°54′W	EC			1999, 2000	1
W	58°40′N	94°40′W	BREB			1990–95	2
SL1	58°40′N	94°40′W	BREB	0.15	0.9	1991, 1995	3, 4
SL2	62°31′N	114°22′W	BREB	0.3	0.6	2000–02	3
SL3	63°35′N	113°54′W	BREB	0.05	3.2	1999–02	3, 5
ML	62°55′N	112°55′W	BREB	5.5	12.1	2000–02	3
LL	61°55′N	113°54′W	EC	18 500	32.2	1997–99	3, 6, 7, 8

Two terrestrial sites are used in this study (Table 3). These are upland, bedrock-dominated terrain of the Canadian Shield, located roughly in the center of the study region (Spence and Rouse 2002) and wetland fen terrain, located in the northern Hudson Bay Lowland (Eaton et al. 2001).

Two years of energy balance data are available from the upland site. It has a surface cover typical of the subarctic shield (Spence and Rouse 2002), with stands of black spruce, mixed stands of spruce and aspen, peat wetlands, and exposed bedrock. There is significant understory vegetation dominated by dwarf birch, Labrador tea, blueberry, and other shrubs.

In the study area wetlands occur in small isolated pockets surrounded by forest and are characteristic of upland terrain. They include sphagnum moss mats overlying organic soils. They are not sufficiently large to allow accurate flux measurements to be undertaken. However, six years of data from an extensive wetland in the Hudson Bay Lowland (Fig. 1) were available. This wetland features hummocky organic terrain comprised of peat underlain by continuous permafrost. The primary vascular vegetation consists of sedges with an extensive nonvascular representation of mosses (Eaton et al. 2001).

The lake sites (Fig. 1) include three small lakes (SL1, SL2, and SL3), one medium lake, and one large lake. The medium lake is Sleepy Dragon Lake and the large lake is Great Slave Lake. In this paper these size and name designations are used interchangeably. The small- and medium-size categories are well represented in the central Mackenzie River basin (Table 1). Large lakes, although more infrequent, are important in terms of total surface area and water volume.

c. Representing lake sizes

It is necessary to address how representative the experimental lakes are of the total lake assemblage (Table 1). Small lakes are well represented by the available data. However, the medium and large lake classes are represented by only one lake each. No data are available for the many lakes in the medium lake category that are substantially larger than Sleepy Dragon. We investigated whether they are best represented by the energy balance established for Sleepy Dragon or the energy balance established for Great Slave Lake. In the study area, these lakes are much closer in surface area to Sleepy Dragon than to Great Slave Lake (Table 2). A comparison of surface temperatures (Bussières and Schertzer 2003) indicates that their temporal cycles (Fig. 2) more closely correspond to that of Sleepy Dragon, and even to the small lakes, than to the cycle of Great Slave Lake. Indeed, more detailed analysis, not presented here, indicates that surface temperature for Gordon Lake, the largest of these lakes (Table 2), mimics Sleepy Dragon patterns quite closely. It is concluded from these comparisons that the energy balance of Sleepy Dragon best represents those lakes classified into the medium lake size category.

d. Measurement and data integrity

The following briefly describes the measurement techniques at the different sites (Fig. 1) and presents estimated errors in the calculation of Q_E and Q_H (Table 4). For the BREB calculations and the Q_E estimate for the upland, potential errors represent root-mean-square (rms) estimates combining each of the component fluxes. For the eddy covariance, they represent estimates of potential errors due to instrumental inaccuracies and site location. Except where otherwise noted, all measurements were recorded on dataloggers (Campbell Instruments, 21X and 23X) and integrated for half-hour periods. The results are presented for daily periods. The techniques at remote sites that could only be visited occasionally (upland, small lakes SL1 and SL2, and medium lake) were dictated by cost and reliability of operation. All instruments were calibrated prior to each field season. All BREB calculations were inspected and corrected using the criteria set out by Ohmura (1982) and Halliwell and Rouse (1989).

When BREB calculations could not be utilized for the lakes due to instrument failure at one or more levels, or vertical gradients that did not exceed the instrumental errors, latent and convective heat fluxes were

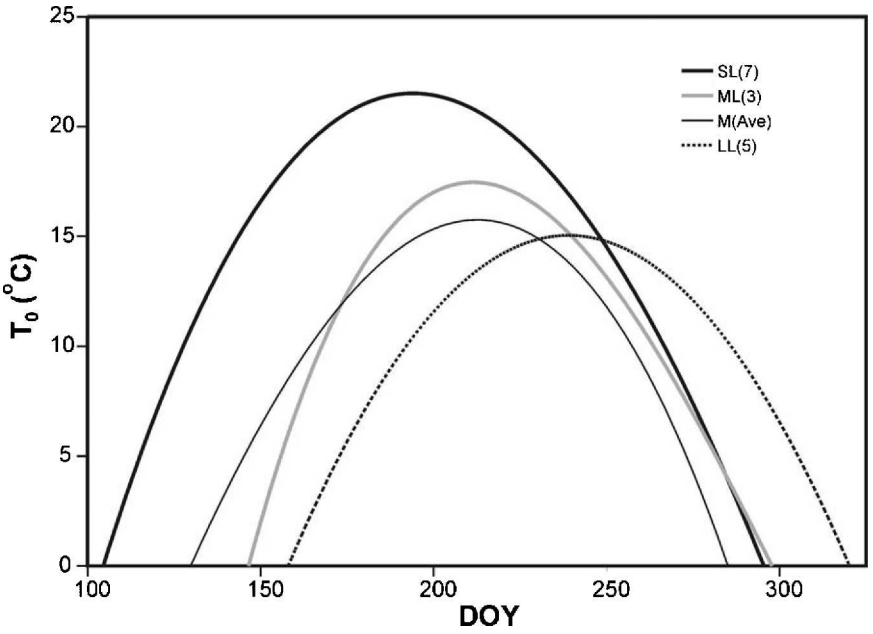

FIG. 2. Third-order polynomials showing seasonal lake surface temperatures for the three categories of lake sizes defined in Table 1. SL, ML, and LL designate small, medium, and large lakes, respectively. The number in parentheses represents the number of years of measurements. Data for other medium lakes [Table 2; M(Ave)] are derived from Bussières and Schertzer (2003).

determined using mass transfer techniques (converted to energy units) where

$$Q_E = m_E u_z \Delta e, \tag{11}$$

$$Q_H = m_H u_z \Delta T. \tag{12}$$

The mass transfer coefficients m_E and m_H are derived at height z over the lake, u_z is the wind speed at height z, and Δe and ΔT are the vapor pressure and temperature differences between height z and the lake surface. Lake surface temperature is derived from the top thermistor in the lake, and the surface vapor pressure is the saturated vapor pressure at the surface temperature. Vapor pressure, temperature, and wind at height z are measured. The mass transfer calculation is made using a daily time unit. The coefficients m_E and m_H are a function of instrument height and the location, size, and shape of the lake. Transfer coefficients determined for a specific lake are not necessarily applicable to other lakes (Oswald and Rouse 2004). Calibration of the mass transfer technique is critical. It requires independent evaporation estimates calculated using tech-

TABLE 4. Instruments and methods used for determining energy balance components and estimated errors are shown. Symbols denote the following: U—upland Canadian Shield terrain; W—wetland; SL1—small lake 1; SL2—small lake 2; SL3—small lake 3; ML—medium lake; LL—large lake; Q^* is net radiation, Q_S is subsurface heat storage, Q_E is latent heat flux, and Q_H is sensible heat flux. EC refers to the eddy covariance method, and BREB to the Bowen ratio-energy balance method of measurement; Φ_E and Φ_H are the estimated errors in determining Q_E and Q_H.

Site	Q^*	Q_S	Q_E	Q_H	Φ_E (%)	Φ_H (%)
U	Net radiometers	Heat flux transducers + calorimetric calculations from thermocouple strings [Eq. (4)]	Residual from Eq. (1)	EC with vertical wind prop and thermocouple	±21	±16
W			BREB with five-level wet- and dry-bulb thermocouple mast		±15	±15
SL		Calorimetric calculations from thermistor string [Eq. (4)]	SL1 and SL2 BREB with three-level thermohygrometer mast; SL3 BREB with three-level thermocouple mast		±18	±18
ML		Calorimetric calculations from thermistor string [Eq. (4)]	Three-level thermohygrometer mast for BREB calculations [Eqs. (6) and (7)]		±20	±20
LL	Net radiometer and component radiation fluxes		Eddy covariance using sonic anemometer, thermocouple, and infrared hygrometer [Eqs. (9) and (10)]		±12	±10

niques such as the BREB or the eddy covariance methods. Missing data over land did not prove a problem.

For the upland site, Q^* was measured continuously from a tower, and periodically over different components of the upland surface. In both cases, the instrument was a Kipp and Zonen NR Lite net radiometer (Spence and Rouse 2002). Spatial variation in Q^* was small. The Fourier heat flow equation was used to estimate Q_G. The vertical temperature gradient was determined from thermistor strings. The heat conduction was based on measurements of the mineral, organic, and water components of the ground; Q_H was measured directly with a vertical propeller anemometer (R. M. Young) coupled with an unshielded copper-constantan thermocouple. Corrections to this measurement are detailed in Spence and Rouse (2002). The error in Q_E as a residual is calculated as the rms of the errors in Q^*, Q_G, and Q_H. At $\pm 21\%$, it has the largest estimated error of any of the components at any of the sites.

At the wetland, Q^* was measured with a Commonwealth Scientific and Industrial Research Organisation (CSIRO) net radiometer. The quantity Q_G was determined using a combination of heat flux transducer measurements and calorimetric calculations, and Q_E and Q_H were derived from BREB calculations. These employed shielded wet- and dry-bulb thermocouples positioned at five heights. Further details of the measurements are given in Eaton et al. (2001).

Measurements at the small (SL1 and SL2) and medium lake sites were very similar. Here Q^* was measured with a Kipp and Zonen NR Lite net radiometer. Lake heat storage, Q_S, was determined as a change in heat storage [Eq. (4)] following the procedure outlined in Oswald and Rouse (2004). The vertical temperature gradients in the lakes were measured using thermistor (Tidbit) strings (one each at small lakes SL1 and SL2, and two at the medium lake). Measurements were integrated over half-hour periods. The atmospheric vertical temperature and humidity gradients for BREB determinations were determined at three heights using shielded air temperature and relative humidity sensors (Vaisala Instruments). At small lake SL3, Q^* was measured with a CSIRO net radiometer (Middleton Instruments); Q_S was determined as for SL1 and SL2, but a thermocouple string was employed. For the BREB calculations, a three-level shielded, wet- and dry-bulb, copper-constantan thermocouple system was utilized, as described in Boudreau and Rouse (1995). Instruments were mounted on floating platforms (SL1, SL2), a small rock outcrop (ML), or a guyed tower in the lake center (SL3).

The Q^* determinations for the large lake employed either a net radiometer (Kipp and Zonen, NR Lite) or were derived from the component fluxes as described in Blanken et al. (2003) and Rouse et al. (2003); Q_S measurements were made calorimetrically. Thermistor (Tidbit) strings were employed to measure lake temperatures, either at one point near the island measurement site (Blanken et al. 2000), or as an average at multiple sites (Schertzer et al. 2003). Heat exchanges Q_E and Q_H were measured directly by eddy covariance [Hydra Mk2, U.K. Hydrological Institute (1997–98); Campbell Scientific Instruments (2001–02)]. Fetch and footprint are of major importance to achieve maximum accuracy and representativeness in measurement. At the upland, considerable care was taken in matching the radiation and eddy covariance footprints so they represent the upland landscape (Spence and Rouse 2002). The wetland site is remarkably uniform over many kilometers, and the upwind fetch is unlimited in all directions (Eaton et al. 2001). For the small and medium lakes, the height of the instruments above the homogeneous lake surface did not exceed 1% of the fetch in any direction. The measurements are considered representative of a fully adjusted boundary layer (Oswald and Rouse 2004). The large lake eddy covariance measurements had unlimited fetch and miminal influence from the island (Blanken et al. 2000).

An error analysis (Table 4) gives a best estimate error based on manufacturer's instrument specifications, documentation, and analysis by other researchers, and a knowledge of site characteristics gained during the various field campaigns (Table 3). There is a range in estimated errors between $\pm 10\%$ for Q_H from the large lake and $\pm 21\%$ for Q_E from the upland. These errors will be examined in terms of the seasonal differences in fluxes from the different surfaces presented in the results section of this study.

Quadratic polynomials are used to extend the seasonal datasets back to the beginning of the ice-free period in spring and forward to the onset of freezing in the fall. Anchoring of these polynomials at either end of the season is aided by lake temperatures from thermistors operating throughout the year, by observation of the end and beginning of freeze, and for the large lake, observations from passive microwave satellite data (Walker et al. 2000).

e. Normalizing data

Since different datasets from different years and locations are compared, it is necessary to normalize all data to a common base. The procedure for this is best explained with an example using small lakes.

- Net radiation Q^* (upland) is used as the common database.
- Common measurement periods for the upland and small lakes are 1999 and 2000 (Table 3).
- Net radiation Q^* (upland) = 75 W m^{-2} averaged for 1999 and 2000 (Table 3). For these 2 yr (Q^*SL)/Q^* (upland) = 1.28.
- Measurements for the three small lakes total 9 yr of data (Table 3).
- Small lake measurements are not available for the periods of thaw and freeze-back. Third-order poly-

TABLE 5. Regional proportions with different terrain combinations are shown; U, W, SL, ML and LL are uplands, wetlands, small lakes, medium lake, and large lake, respectively.

Landscape combinations	Regional proportions				
	U	W	SL	ML	LL
U	1.00				
U + W	0.87	0.13			
U + W + SL	0.79	0.11	0.10		
U + W + SL + ML	0.67	0.10	0.09	0.14	
U + W + SL + L + LL	0.55	0.08	0.07	0.11	0.19

nomials are used to extend the data to the start of melt and the end of freeze-back. This gives a seasonal curve for each flux.

- Integration of the seasonal curves allows the following ratios to be calculated:

$$Q_S(\mathrm{SL})/Q^*(\mathrm{SL}) = 0.02,$$

$$Q_E(\mathrm{SL})/Q^*(\mathrm{SL}) = 0.62,$$

$$Q_H(\mathrm{SL})/Q^*(\mathrm{SL}) = 0.36.$$

Applying these ratios to seasonal averages prorated to the common data period (1999, 2000) gives

$$Q^*(\mathrm{SL}) = 75 \times 1.28 = 96,$$

$$Q_S(\mathrm{SL}) = 96 \times 0.02 = 2,$$

$$Q_E(\mathrm{SL}) = 96 \times 0.62 = 60,$$

$$Q_H(\mathrm{SL}) = 96 \times 0.36 = 34.$$

Normalization also allows extraction of daily average values.

Other surfaces are treated in a similar manner. Since they are in a different geographical location, and for different years, the wetland measurements were related to the nearby small lake (SL3) for common time periods. They were then prorated to Q^* (upland) using the small lake relationships developed above.

3. Results

The discussion of results refers exclusively to the normalized dataset. "Season" or "seasonal" as used in this study extends from the start of the thaw period in the upland (23 April) to the final freeze of the large lake (14 January). The division into first and second halves of the season occurs on 2 September [day of year (DOY) 245]. The results are presented in the following format. Examples of annual radiation cycles are presented to illustrate the seasonal patterns. Solar and net radiation are introduced next. Their differences between surfaces are fundamental to the regional energy balance. The other component energy fluxes are then examined. The regional energy balances, resulting from different landscape combinations (Table 5) are developed next. Finally we assess the significance of lake size to the regional energy balance.

a. Annual cycles

Figure 3 illustrates the annual cycle of incoming solar radiation at Yellowknife, Northwest Territories ($K\downarrow$YK), and net radiation for Great Slave Lake (Q^*LL) and the upland (Q^*U) . The solar radiation data have been derived using a radiation transfer model (Davies and McKay 1982). The net radiation curves have been derived using all measured data. The time periods for the three sets of data do not totally coincide and hence are not directly comparable quantitatively. Also, winter measurements are often unreliable.

The general patterns show distinctive annual cycles. Because of the high-latitude location, $K\downarrow$YK ranges from large input at the summer solstice to near zero at the winter solstice. In early spring, positive Q^*U begins when $K\downarrow$YK has achieved daily averages of 220 W m^{-2} in late April (DOY 112), but the onset of positive Q^*LL lags until $K\downarrow$YK has achieved daily averages of 255 W m^{-2} in mid-May (DOY 133). In early winter, negative Q^*U begins when $K\downarrow$YK has decreased to 60 W m^{-2} at the beginning of October (DOY 274), but the onset of negative Q^*LL lags until $K\downarrow$YK has decreased to 25 W m^{-2} in mid-October (DOY 289) In spring, the large time lags of net radiation behind increasing solar radiation are due to the longevity of the high albedo snow cover on the upland and even greater longevity of the snow and ice cover on Great Slave Lake. In early winter, the extended period of positive net radiation over the lake compared to the upland is due to the maintenance of open water (small surface albedo) until well after the land is snow covered.

b. Radiation balances

Net radiation Q^* is substantially greater over all water-dominated surfaces than for the upland. Relative to the upland, seasonal Q^* is 16% greater for wetland, about 25% greater for small and medium lakes, and 73% greater for Great Slave Lake. Albedo, as it decreases with increasing surface wetness, plays a primary role in determining differences in Q^* between surfaces.

The large Q^* over Great Slave Lake, relative to the other surfaces, is consistent over a number of years of measurement. Three summers of comparable data (Table 6) indicate that Q^* at Great Slave Lake is greater than that measured at Sleepy Dragon Lake, which is located 100 km inland (ML, Fig. 1). This is due to clearer daytime skies during the summer period.

Figure 4 compares clear-sky conditions over Great Slave Lake with those centered 100 km inland at Sleepy Dragon Lake. These data are derived using the National Oceanic and Atmospheric Administration (NOAA) Advanced Very High Resolution Radiometer (AVHRR) 1.25-km cloud mask. This is a binary technique that indicates that the sky is either clear or

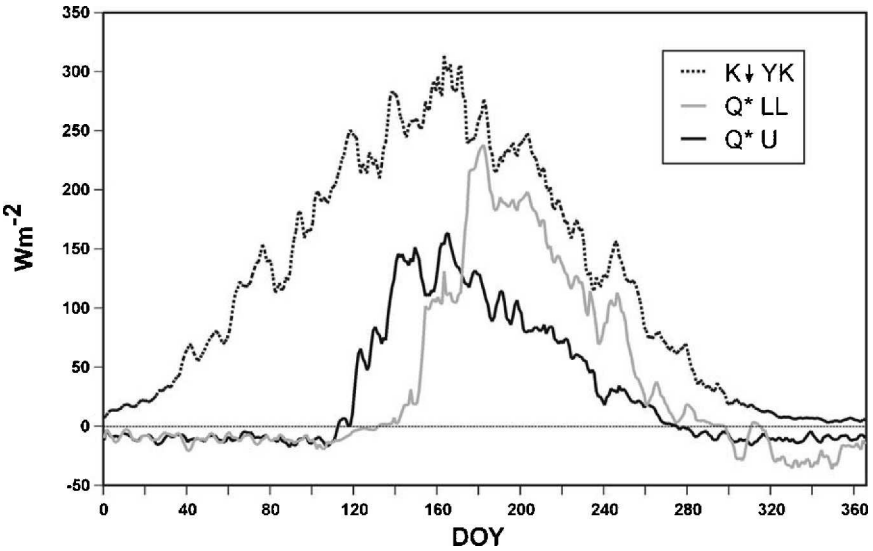

FIG. 3. Annual radiation cycles. Incoming solar radiation at Yellowknife ($K\downarrow$YK) is calculated from a radiation transfer model (Davies and Hay 1980). Net radiation for Great Slave Lake (Q^*LL) and upland (Q^*U) employs all available measured data. It is presented as 5-day running means. The station locations are shown in Fig. 1.

cloudy. It does not denote percent cloudiness. In spring (April–May–June), the frequency of relatively clear skies is similar in early morning (0400 LT) and early afternoon (1400 LT). In summer (June–July–August), morning clear skies are similar but the afternoon clear-sky condition persists 64% of the time over Great Slave Lake and 38% over Sleepy Dragon Lake. These clearer skies are a response to the stable atmosphere over Great Slave Lake and are the primary cause of larger $K\downarrow$ and Q^*. Table 6 indicates that the net longwave loss (L*) from the large and medium lake is similar (Table 6). The large lake has both smaller outgoing longwave and smaller incoming longwave radiation. The former is due to colder radiative surface temperatures. The latter is a result of colder near-surface air temperatures and lesser cloud cover.

Seasonal cumulative curves are computed by adding the daily fluxes from the beginning to the end of the season. The temporal pattern (Fig. 5) shows the following. There is a lag in achieving positive Q^* at the beginning of the snow-free season. Upland and wetland respond similarly, showing a positive Q^* by 1 May (DOY 121). The lag in achieving positive Q^* over lakes is controlled by the extent of lake ice melt. Small lakes lag by about 1 week and medium and large lakes by 3 weeks. Net radiation Q^* accumulates at similar rates for all surfaces (Fig. 5). The end of positive Q^* for upland occurs on 27 September (DOY 270) and for wetland on 28 September (DOY 271). The end of positive Q^* for small lakes occurs on 7 October (DOY 280), for the medium lake on 21 October (DOY 294), and for the large lake on 14 October (DOY 287).

TABLE 6. Comparative fluxes for the large (LL) and medium (ML) lakes are presented. The fluxes are based on common summer data periods for 2000, 2001, and 2002, where $K\downarrow$, $K\uparrow$, and K^* are incoming, reflected, and net solar radiation, respectively; T_0 is water surface temperature (°C); $L\uparrow$, $L\downarrow$, and L^* are outgoing, incoming, and net longwave radiation, respectively; Q^* is net radiation; and flux values are in W m^{-2}.

	$K\downarrow$	$K\uparrow$	Albedo	K^*	T_0	$L\downarrow$	$L\uparrow$	L^*	Q^*
LL	234	14	0.06	220	9.7	308	252	−44	177
ML	204	12	0.06	192	15.2	335	381	−46	146

c. *Comparative energy balances of individual surfaces*

The small albedo of lakes implies that solar radiation penetrates into and is absorbed by the water. Worth (2002) found that as a summer average, central Great Slave Lake absorbs 79% of photosynthetically active solar radiation in the upper 2 m of the lake. The medium lake absorbed 53%, and one of the small lakes 98% in this layer. The depth of penetration and zone of radiational heating depends on dissolved organic content and turbidity due to suspended particulates.

After absorption, the energy is mixed within the lake waters by forced and free convection. Small and shallow lakes mix thoroughly, resulting in uniform temperatures throughout most of their depths. At the end of summer, mixing depths are about 10 and 18 m, respectively, for the medium and large lake in this study (Oswald and Rouse 2004). The heat storage of lakes is large compared to terrestrial surfaces (Fig. 5). In our study, the maximum seasonal heat storages (MJ m^{-2}) were upland (57), wetland (91), small lakes (258), medium lake (562), and large lake (1048). Upland, wet-

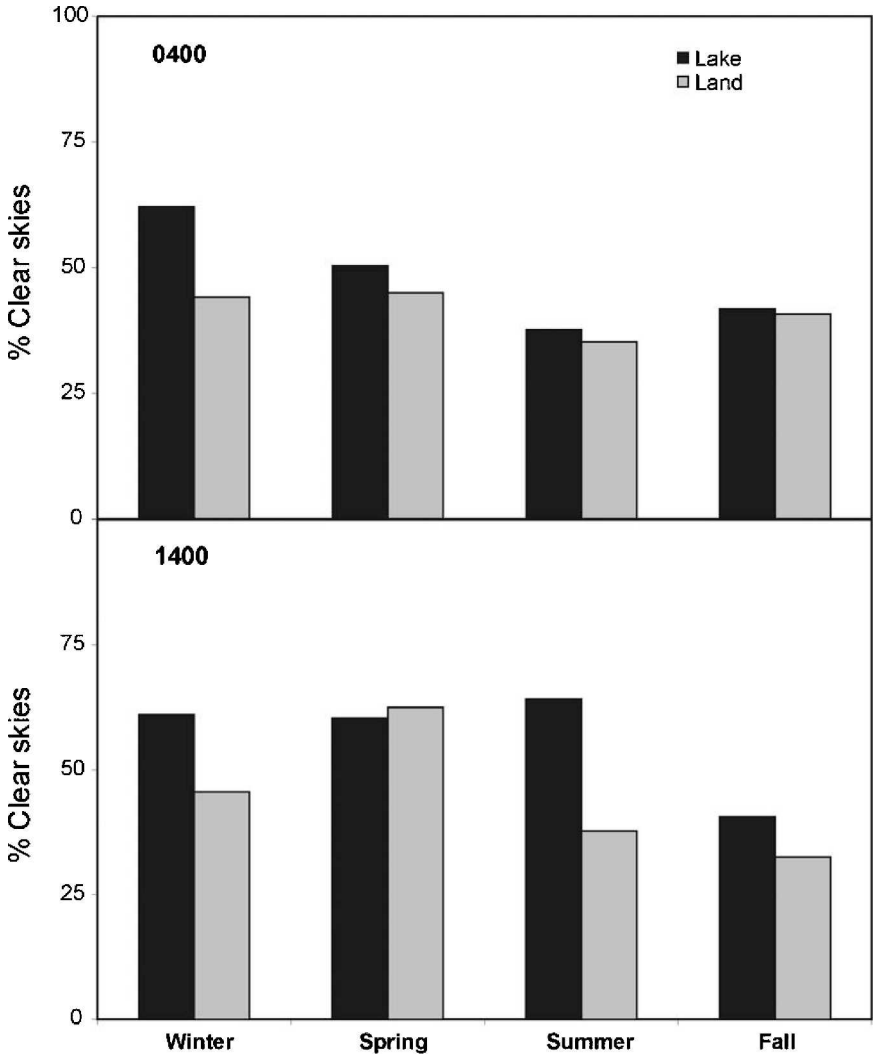

FIG. 4. Seasonal percentage of relatively clear skies as determined over Great Slave Lake (Lake) and the inland terrestrial area (Land) 100 km to the northeast of Yellowknife. Local times of 0400 and 1400 h are centered for a 3-h time frame of NOAA/AVHRR satellite transmission.

land, and small lakes reached their maximum heat storage about 1 August (DOY 213). The medium and large lake reached it on 6 August (DOY 218) and 8 September (DOY 249), respectively. At the time of maximum heat storage, (Q_S/Q^*) is as follows: upland (0.06), wetland (0.09), small lakes (0.26), medium lake (0.55), and large lake (0.76). Thus, depending on lake size, by late summer, from one-quarter to three-quarters of the available radiant energy has gone into heating the lakes.

The large heat storage in lakes near summer's end has a major impact on the regional energy balance, because this energy is utilized to drive convective heat fluxes in fall and early winter. This is evident in the latent (Q_E), sensible (Q_H), and combined ($Q_E + Q_H$) convective heat fluxes (Fig. 5). The Q_E for upland, wetland, and small lakes is similar until mid-July when the bedrock-dominated uplands become quite dry (Spence and Rouse 2002) and evaporation becomes small. The Q_E for wetland and small lakes continues at the same rates until 9 September (DOY 252). At this time, wetlands largely cease evaporating because of small Q^* and freezing temperatures. Small lakes continue to evaporate until the end of September, utilizing their stored energy.

The medium and large lakes show substantially different behavior. The commencement of evaporation lags 5 to 6 weeks behind that of upland and wetland. The medium lake then exhibits evaporation rates comparable to wetland and small lakes throughout most of the summer. However, these high rates persist into early November, about 3 weeks after small lakes have

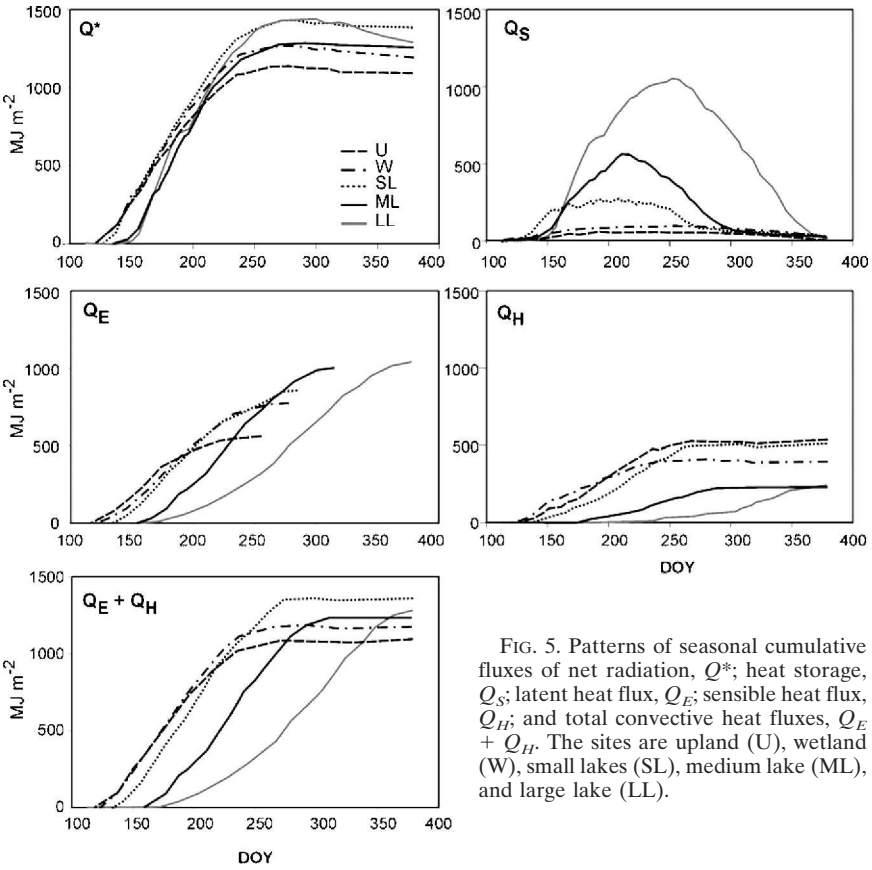

FIG. 5. Patterns of seasonal cumulative fluxes of net radiation, Q^*; heat storage, Q_S; latent heat flux, Q_E; sensible heat flux, Q_H; and total convective heat fluxes, $Q_E + Q_H$. The sites are upland (U), wetland (W), small lakes (SL), medium lake (ML), and large lake (LL).

frozen and ceased evaporating. The large lake undergoes relatively slow evaporation rates until mid-September, after which the rates accelerate (Rouse et al. 2003). The Q_E remains positive into early January before Great Slave Lake fully freezes. The large heat storage in medium and large lakes sustains major Q_E into the fall and winter period when Q^* has become negligible or negative. The number of weeks of evaporation are as follows: upland (19), wetland (21), small lakes (22), medium lake (24), and large lake (30). For Great Slave Lake the evaporation period exceeds the totally ice free period. Evaporation can start before that lake totally thaws in early summer. In early winter, the main part of the lake evaporates vigorously when ice is forming in the shallower coastal zones and bays.

The cumulative seasonal patterns for Q_H are similar to those for Q_E with similar lags at the beginning and end of the season (Fig. 5). Total Q_H for upland and small lakes is about one-third greater than for the wetland, and about double that for the medium and large lakes. The relatively large Q_H from the upland results from the dry surface, which gives a large Bowen ratio (Spence and Rouse 2002). The relatively large Q_H for small lakes is due to two factors. First, the rapid warming early in the season (Q_S; Fig. 5) promotes steep temperature gradients over the lake, especially at night and during cold-air outbreaks. This favors a substantial sensible heat flux. Second, near the end of the open-water period, the residual stored heat spawns steep vertical temperature gradients. This enhances Q_H. The Q_H from the medium and large lakes is suppressed by inversion temperature gradients over the lakes during the spring and summer periods (Rouse et al. 2003). For the large lake, during this inversion period, Q_E is sustained by periodic disturbances that entrain heat energy from above the surface boundary layer (Blanken et al. 2003).

The combined heat fluxes ($Q_E + Q_H$; Fig. 5) clearly indicate the importance of lakes in augmenting the convective heat fluxes into the atmosphere, particularly in fall and early winter.

d. Comparative regional energy balances

The effects of combinations of surface types is facilitated by treating the region (Fig. 1; Table 1) as comprising uplands only, then sequentially adding the influence of wetlands, small lakes, medium lake, and large lake, with the regional proportions shown in Table 5. Because of the large seasonal difference in the energy balance of the different surface types, an understanding of the important processes is facilitated by dividing the results into a first (early) half and second (late) half. The division date between early and late

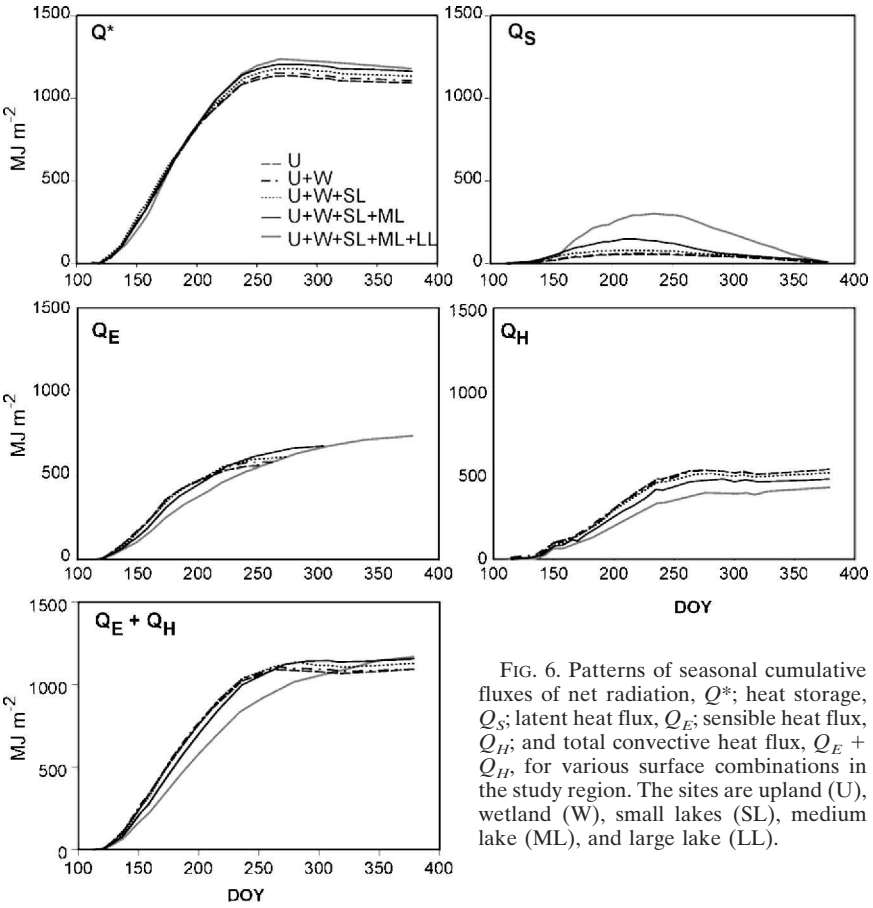

FIG. 6. Patterns of seasonal cumulative fluxes of net radiation, Q^*; heat storage, Q_S; latent heat flux, Q_E; sensible heat flux, Q_H; and total convective heat flux, $Q_E + Q_H$, for various surface combinations in the study region. The sites are upland (U), wetland (W), small lakes (SL), medium lake (ML), and large lake (LL).

season (2 September; DOY 245) corresponds closely to the time when air temperatures over Great Slave Lake and the adjacent mainland equalize (Rouse et al. 2003). It is also the changeover time from increasing to decreasing air temperatures.

The addition of wetlands and lakes to the region enhances Q^* by 8%, an increase that is relatively uniform throughout the season (Fig. 6). Lakes increase the maximum heat storage, Q_S, more than fourfold (Table 7; early season). Seasonal Q_E is increased by 32%, which incorporates a small decrease in the first half and a large sixfold enhancement in the second half. Seasonal Q_H is decreased by 19%, all of which occurs early in the first half. It is evident (Fig. 6) that medium and large lakes are the most important surface types in enhancing regional latent heat flux, Q_E, and the combined convective heat fluxes ($Q_E + Q_H$) into the atmosphere.

e. The significance of comparative energy balance data

Percent differences in seasonal Q_E and Q_H (Table 8) can be examined in light of estimated measurement errors (Table 4). This helps to assess the significance of these differences. Differences between upland and all other surfaces are substantially larger than potential errors. These are considered significant. Differences in Q_E between wetlands and small lakes are smaller than estimated errors and are considered insignificant. The Q_H for the small lakes is substantially larger than for the wetland. This difference arises from greater Q^*, which is a significant calculation; hence the larger Q_H is considered significant. The medium and large lakes stand in a class of their own, with significantly greater Q_E and lesser Q_H than either the upland, wetland, or small lakes. Differences in seasonal magnitudes between the medium and large lakes are smaller than the potential errors in calculation. They are considered insignificant. However, since the large lakes thaw and freeze later than medium ones, differences in the timing of the fluxes are significant.

f. Importance of lake size

A question for regional modeling is whether all lakes can be treated the same and simply represented by their surface area. Another way of phrasing this is with the following question: Does an equal area composite of small lakes give similar results as a lesser number of medium lakes or one large lake? The foregoing evidence indicates that small lakes behave differently from medium and large lakes.

TABLE 7. Energy balance relationships. (a) Energy fluxes (MJ m^{-2}) during the first half of the season (early), the second half (late), and seasonal totals (seasonal). (b) The ratio of early- and late-season fluxes to seasonal. (c) The ratio of [(upland + lake category)/upland]. Here Q^* is net radiation, Q_S is heat storage, Q_E is latent heat flux, and Q_H is sensible heat flux; U, W, SL, ML, and LL designate uplands, wetlands, small lakes, medium lake, and large lake, respectively.

	Early season				Late season			
Days	134				134			
(a) Fluxes	Q^*	Q_S	Q_E	Q_H	Q^*	Q_S	Q_E	Q_H
U	933	57	509	367	161	−57	51	167
U + W	944	61	520	363	163	−58	67	154
U + W + SL	960	81	527	352	175	−75	86	164
U + W + SL + ML	972	149	509	314	192	−140	166	166
U + W + SL + ML + LL	973	286	433	254	205	−278	305	178
	(b) Ratio to seasonal total							
U	0.85	*	0.91	0.69	0.15	*	0.09	0.31
U + W	0.85	*	0.89	0.70	0.15	*	0.11	0.30
U + W + SL	0.85	*	0.86	0.68	0.15	*	0.14	0.32
U + W + SL + ML	0.84	*	0.75	0.65	0.16	*	0.25	0.35
U + W + SL + ML + LL	0.83	*	0.59	0.59	0.17	*	0.41	0.41
	(c) Ratio to upland							
U	1	1	1	1	1	1	1	1
U + W	1.01	1.07	1.02	0.99	1.01	1.02	1.33	0.92
U + W + SL	1.03	1.40	1.04	0.96	1.09	1.32	1.69	0.98
U + W + SL + ML	1.04	2.61	1.00	0.86	1.19	2.46	3.25	0.99
U + W + SL + ML + LL	1.04	5.01	0.85	0.69	1.27	4.86	5.98	1.07

* Seasonal total of $Q_S \rightarrow 0$ so ratio loses meaning.

This idea can be further examined by comparing a region of uplands and wetlands only (i.e., no lakes) to one in which the 37% lake proportion of the landscape is totally occupied by small lakes, medium lakes, or large lakes. Figure 7 presents the resulting degree of change. The various combinations indicate little change in regional Q^* and little skewing in its seasonal distribution. The Q_H from a small lake composite is about 20% greater than for medium and large lake composites. This difference all occurs in the first half of the open-water season. For the small lake composite, Q_E averages 9% less than for its medium and large lake counterparts. All of the difference occurs in the second half of the open-water season. There is little difference in the combined heat fluxes $Q_E + Q_H$ over the full season, but there is a substantial seasonal skewing. The small lake composite gives about 20% greater magnitude in the first half and 63% less magnitude in the second half of the season, respectively.

TABLE 8. Differences (percent) in the seasonal convective heat fluxes between surfaces are presented. Differences in latent heat flux (Q_E) are shown in bold in the upper right-triangle and differences in sensible heat flux (Q_H) in italics in the lower-left triangle; U, W, SL, ML, and LL designate uplands, wetlands, small lakes, medium lake, and large lake, respectively.

	U	W	SL	ML	LL
U	—	**39**	**46**	**80**	**88**
W	*−48*	—	**5**	**30**	**35**
SL	*−32*	*32*	—	**23**	**35**
ML	*−70*	*−42*	*−56*	—	**6**
LL	*−75*	*−53*	*−53*	*−11*	—

4. Discussion

The implications of the results of this study can be considered at several scales. The enhancement of latent heat flux and suppression of sensible heat flux, due to the insertion of lakes into a landscape, is consistent with the findings of Bonan (1995) and Nagarajan et al. (2004). A number of studies indicate that evaporation is an important source for precipitation within the Mackenzie River basin (MRB). Walsh et al. (1994) report that during the summer season, evaporation from the MRB is a significant source of moisture. Szeto (2002) calculates that the highest recycling ratios (fraction of precipitation that is derived from evaporation within the basin) are found over the eastern part of the MRB during the warm season. He attributes this, in part, to large evaporation from the extensive lake and wetland systems. Unfortunately, precipitation measurements are so sparse in this region that the contribution of lakes is impossible to document from direct measurement. There is some evidence from passive microwave satellite images that the larger lakes contribute to enhanced downwind snowfalls, but no substantive studies have yet been pursued on this feature. It is well documented that the Laurentian Great Lakes result in enhanced downwind snowfall. Since early winter conditions are similar for Great Slave Lake and other large lakes (i.e., large late-season evaporation and frozen upland surfaces with substantial relief that contribute to low-level condensation) one can speculate that downwind snowfall will be enhanced. It is a study that needs

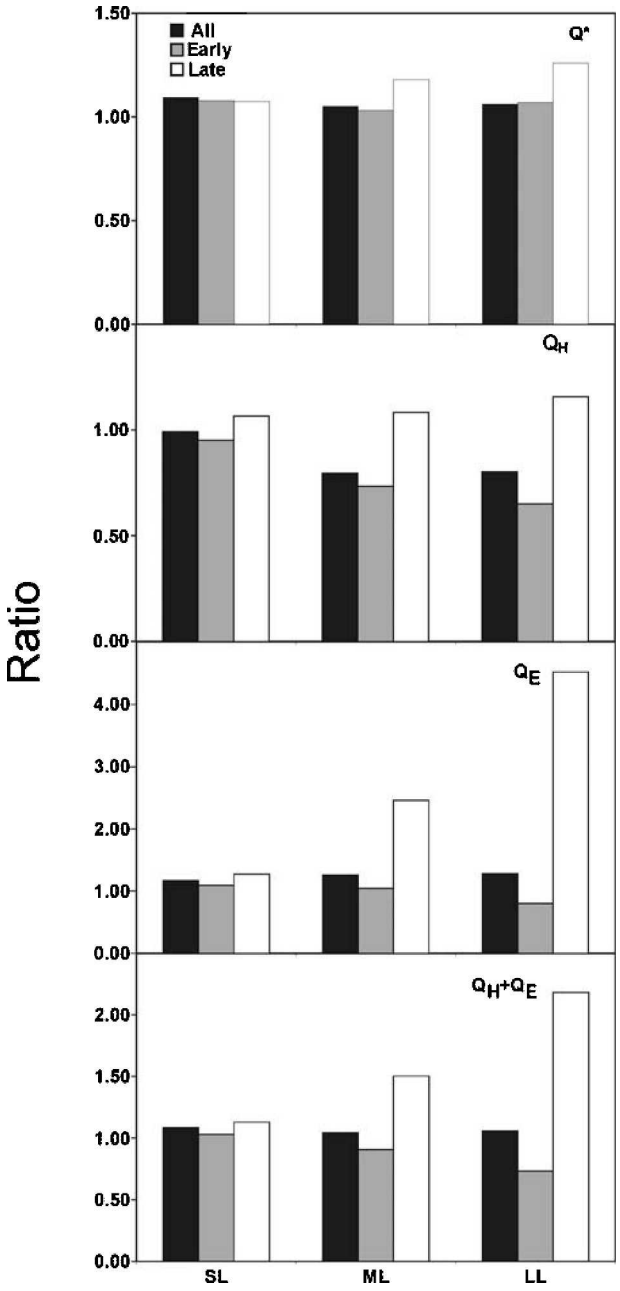

FIG. 7. The influence of size of lake on the regional energy balance, where Q^*, Q_H, Q_E, and $Q_E + Q_H$ are net radiation, sensible heat flux, latent heat flux, and total convective heat fluxes, respectively. Ratio = x/y, where x specifies the energy balance component with one only of the lake types represented in the 37% lake portion of the region, and y represents the energy balance component for the region with no lakes (i.e., only uplands + wetlands).

to be pursued because it can have significant regional hydrological impacts.

This study has shown that lake size is important to the magnitude of regional energy balances. Future research is needed into the role of lake depth and the clarity of water, particularly as it affects heat storage. Three examples indicate that this is a complex problem. These examples are Great Slave Lake (LL), Sleepy Dragon Lake (ML), and a small lake (SL2). Their depths at the measurement sites are 61, 32, and 7 m, respectively. Their opacities range from low (ML) to quite high (LL, SL2). At the end of the summer heating period, the depths of their thermoclines, which represent the main zones of heat storage, are LL (18 m), ML (10 m), and SL2 (3m). Great Slave Lake (LL) is quite turbid and most of the solar radiation is absorbed within 2.5 m of its surface. However, it heats to substantial depths. This deep heating is due to large upwind fetches, large wind shear, and vigorous wind-driven mechanical mixing, particularly during storms. In this example, large size is more important to heat storage than depth of penetration of solar radiation.

Sleepy Dragon Lake (ML) is substantially clearer than Great Slave Lake or SL2. Its thermocline depth lies between these two extremes. In this example, size appears to be more important to heat storage than is clarity.

For the small lake, all of the solar radiation is absorbed in the top 2.5 m of water and there is little mechanical mixing because of its small surface area and limited wind fetch. In this example, both lake size and water clarity limit the depth of heat storage. Evidently size alone is of major importance due to its control on wind fetch and mechanical mixing.

5. Conclusions

In lake-rich high-latitude regions, lakes play an important role in the regional energy balance. They are high-energy systems compared with terrestrial landscapes. This arises mainly because of their ability to transmit and absorb solar radiation. In this study, the net radiation of lakes during the open-water season is anywhere from 25% to 73% greater than for upland surfaces in the region. The largest net radiation in our study occurred on Great Slave Lake. The prevalence of stable atmospheric conditions helps suppress cloud cover and enhances the magnitude of incoming solar radiation. The addition of wetlands and lakes to the study region enhances net radiation by 8% above that for uplands alone. During the long daylight periods of summer, the larger the lake the greater its heat storage. By late summer, depending on lake size, from one-quarter to three-quarters of the available radiant energy has gone into heating the lakes. This keeps the larger lakes ice-free into fall and early winter. The regional heat storage at maximum is increased more than fourfold over the value for uplands alone. In the medium and large lakes, this storage has a major impact on the regional energy balance. It results in large convective heat fluxes in the second half of the season. Full-season regional evaporation (latent heat flux) is increased by 32% compared with uplands alone. This incorporates a small decrease in the first half of the

season and a sixfold enhancement in the second half. Full-season sensible heat flux is decreased by 19%, all of which occurs in the first half. For energy budget modeling purposes the representation of lake size is important. Net radiation is fairly independent of size. Compared with medium and large lakes, an equal area composite of small lakes yields substantially greater regional sensible heat flux and lesser latent heat flux. Additionally, there are large regional differences in the early- and late-season energy balance and evaporation amounts resulting from lake size.

Acknowledgments. Financial support for this project was provided by network research grants from the Meteorological Service of Canada (MSC) and the Natural Science and Engineering Research Council of Canada (NSERC) provided to the Mackenzie GEWEX Study, individual NSERC research grants, a research grant from NASA, USA, and Student Northern Training Grants from the Canada Department of Indian and Northern Affairs. Logistical and equipment support during measurement campaigns has been provided by the Great Slave Lake branch of the Canadian Coast Guard; Environment Canada, Yellowknife, Northwest Territories; Institute of Hydrology, Wallingford, United Kingdom; MSC, Toronto, Ontario; National Water Research Institute, Burlington, Ontario; Royal Canadian Mounted Police Marine Unit, Yellowknife, Northwest Territories; Water Survey of Canada, Yellowknife, Northwest Territories; and Churchill Northern Studies Centre, Churchill, Manitoba. Lake thaw and freeze-up data have been provided by Ann Walker, MSC. Bob Kochtubajda, Environment Canada, Edmonton, facilitated obtaining appropriate meteorological data. Patrick Ménard, Toronto, did the satellite cloud analysis and compilation. Many graduate students and technical support staff have been involved in the various field campaigns and our thanks go to all of them.

REFERENCES

Bello, R., and J. D. Smith, 1990: The effect of weather variability on the energy balance of a lake in the Hudson Bay Lowlands, Canada. *Arct. Alp. Res.,* **22,** 98–107.

Blanken, P. D., and Coauthors, 2000: Eddy covariance measurements of evaporation from Great Slave Lake, Northwest Territories, Canada. *Water Resour. Res.,* **36,** 1069–1078.

——, W. R. Rouse, and W. M. Schertzer, 2003: The enhancement of evaporation from a large northern lake by the entrainment of warm, dry air. *J. Hydrometeor.,* **4,** 680–693.

Bonan, G. B., 1995: Sensitivity of a GCM simulation to inclusion of inland water sources. *J. Climate,* **8,** 2691–2704.

Boudreau, L. D., and W. R. Rouse, 1995: The role of individual terrain units in the water balance of wetland tundra. *Climate Res.,* **5,** 31–47.

Bussières, N., 2002: Thermal features of the Mackenzie Basin from multiple NOAA AVHRR sensor observations for summer 1994. *Atmos.–Ocean,* **40,** 233–244.

——, and W. M. Schertzer, 2003: The evolution of AVHRR-derived water temperatures over lakes in the Mackenzie Basin and hydrometeorological applications. *J. Hydrometeor.,* **4,** 660–672.

Davies, J. A., and D. C. McKay, 1982: Estimating solar irradiance and components. *Sol. Energy,* **29,** 55–64.

Eaton, A. K., W. R. Rouse, P. M. Lafleur, P. Marsh, and P. D. Blanken, 2001: Surface energy balance of the western and central Canadian subarctic: Variations in the energy balance among five major terrain types. *J. Climate,* **14,** 3692–3703.

Halliwell, D. H., and W. R. Rouse, 1989: A comparison of sensible and latent heat flux calculations using the Bowen ratio and aerodynamic methods. *J. Atmos. Oceanic Technol.,* **6,** 563–574.

Nagarajan, B., M. K. Yau, and P. H. Schuepp, 2004: The effects of small water bodies on the atmospheric heat and water budgets over the Mackenzie River Basin. *Hydrol. Processes,* **18,** 913–938.

Ohmura, A., 1982: Objective criteria for rejecting data for Bowen ratio flux calculations. *J. Appl. Meteor.,* **21,** 595–598.

Oswald, C. M., and W. R. Rouse, 2004: Thermal characteristics and energy balance of various-size Canadian Shield lakes in the Mackenzie River Basin. *J. Hydrometeor.,* **5,** 129–144.

Petrone, R., and W. R. Rouse, 2000: Synoptic controls on the surface energy and water budgets in subarctic regions in Canada. *Int. J. Climatol.,* **20,** 1149–1165.

Rouse, W. R., R. L. Bello, and P. M. Lafleur, 1997: Boreal, subarctic and low Arctic. *The Surface Climates of Canada,* W. G. Bailey, T. R. Oke, and W. R. Rouse, Eds., McGill-Queens Press, 198–221.

——, C. J. Oswald, C. Spence, W. M. Schertzer, and P. D. Blanken, 2002: *Cold Region Lakes and Landscape Evaporation. Proceedings of the 2nd GAME-MAGS Joint International Workshop,* P. diCenzo and L. W. Martz, Eds., GEWEX-MAGS Secretariat, 37–42. [Available from MAGS Secretariat, NWRI, Saskatoon, S7N 3H5, Canada.]

——, C. M. Oswald, J. Binyamin, P. D. Blanken, W. M. Schertzer, and C. Spence, 2003: Interannual and seasonal variability of the surface energy balance and temperature of Central Great Slave Lake. *J. Hydrometeor.,* **4,** 720–730.

Schertzer, W. M., 1997: Freshwater lakes. *The Surface Climates of Canada*, W. G. Bailey, T.R. Oke, and W. R. Rouse, Eds., McGill-Queens University Press, 124–148.

——, 2000: Digital bathymetry of Great Slave Lake. NWRI Contribution 00-257, National Water Research Institute, Burlington, ON, Canada, 46 p.

——, W. R. Rouse, and P. D. Blanken, 2000: Cross-lake variation of physical limnological and climatological processes of Great Slave Lake. *Phys. Geogr.,* **21,** 385–406.

——, ——, ——, and A. E. Walker, 2003: Over-lake meteorology, thermal response, heat content and estimate of the bulk heat exchange of Great Slave Lake During CAGES (1998–1999). *J. Hydrometeor.,* **4,** 649–659.

Spence, C., and W. R. Rouse, 2002: The energy budget of Canadian Shield subarctic terrain and its impact on hillslope hydrology. *J. Hydrometeor.,* **3,** 208–218.

——, ——, C. M. Oswald, D. Worth, and B. Reid, 2003: The energy budget of a small Canadian Shield lake. *J. Hydrometeor.,* **4,** 694–701.

Szeto, K. K., 2002: Moisture recycling over the Mackenzie Basin. *Atmos.–Ocean,* **40,** 181–197.

Walker, A., A. Silis, J. R. Metcalf, M. R. Davey, R. D. Brown, and B. E. Goodison, 2000: Snow cover and lake ice determination in the MAGS region using passive microwave satellite and conventional data. *Proceedings of the Fifth Scientific Workshop for the Mackenzie GEWEX Study*, G. S. Strong and Y. M. L.Wilkinson, Eds., MAGS Secretariat, 39–42. [Available from MAGS Secretariat, NWRI, Saskatoon, SK, S7N 3H5, Canada.]

Walsh, J. E., X. Zhou, D. Serreze, and M. C. Serreze, 1994: Atmospheric contributions to hydrologic variations in the Arctic. *Atmos.–Ocean,* **32,** 733–755.

Worth, D. E., 2002: The reflection and attenuation of light in subarctic lakes. M.Sc. thesis, McMaster University, Hamilton, ON, Canada, 127 pp.